# The Electric Vehicle Model (EVM): A novel car-following model for electric adaptive cruise control vehicles

Arian Zare, Mingfeng Shang, Student Member, IEEE, Xingan (David) Kan, and Raphael Stern, Member, IEEE

Abstract—Electric vehicle (EV) adoption is accelerating across the automotive industry. The first generation of electrified vehicles with driver assistance features like adaptive cruise control (ACC) are now commercially available. While studies have highlighted the sustainability benefits of EVs, recent research suggests these EVs may impact traffic flow differently than traditional internal combustion engine (ICE) vehicles since they have distinct driving dynamics. Understanding the differences between EV-ACC and ICE-ACC vehicle driving behaviors and their effects on traffic flow remains an important research gap.

To address this gap, we leverage a recently published EV-ACC dataset and develop a new microscopic car-following model, namely the electric vehicle model (EVM), to understand EV-ACC driving behavior. The proposed model is calibrated using batch optimization and outperforms other commonly used car-following models in capturing EV-ACC car-following patterns. Moreover, we use a simulation of a string of EV-ACC vehicles behaving based on the parameter values of the EVM model to demonstrate their ability to reduce traffic oscillations compared to the commonly used car-following models.

#### I. INTRODUCTION

The transportation industry has undergone a rapid revolution with the emergence of autonomous vehicles (AVs). As several researches have demonstrated, the behavior of AVs can significantly impact traffic flow patterns. Even a low penetration rate of AVs can significantly improve highway traffic flow stability [1]. Moreover, the existence of AVs in the traffic flow can notably reduce the velocity standard deviation, excessive braking, and fuel consumption [2]. We are still far from a fully AV environment on roads. However, the automotive industry is increasingly shifting towards selling vehicles equipped with advanced driver assistance systems and greater levels of automation. For example, over the past few decades, advanced driver assistance systems (ADAS) such as adaptive cruise control (ACC) (e.g., SAE Level 1-2) [3], have become popular in the market and the majority of vehicles are now equipped with this technology. Stringstable traffic flow [4], increased highway throughput [5], and decreased fuel consumption and emissions [6] are outcomes of a network with fully AVs. However, recent studies suggest these benefits may not exhibit commercially available ACC vehicles. For example, Shang and Stern [7] find commercially available ACC vehicles can reduce highway throughput. Through simulation, Vander Werf et al. [8] show that ACC systems can reduce highway capacity by up to 25% when ACC vehicles constitute 15-30% of the traffic stream.

In parallel with vehicle automation advancements, the demand for cleaner and more efficient transportation continues to grow. Electric vehicles (EVs) are becoming increasingly popular and gradually taking over the market from the traditional internal combustion engine (ICE) vehicles. Current EVs are equipped with a wide range of advanced features, including ACC.

Though many aspects of EVs and ICE vehicles are similar, there are major mechanical differences. ICE vehicles gradually increase torque and require high engine speeds for maximum power output, while EVs can produce high torque instantly from low speeds. This allows EVs to accelerate faster at typical low speeds. Additionally, EVs utilize regenerative braking for stronger deceleration capabilities. As a result, EV-ACC vehicles are more reactive in oscillatory traffic conditions, with the potential to drive at shorter following distances and accelerate more quickly than ICE-ACC vehicles.

Dating back to the 1950s [9], numerous microscopic carfollowing models have been developed using differential equations to accurately describe individual vehicle driving behavior and examine the traffic flow through simulations [10]. These models have captured different realistic traffic phenomena like stop-and-go waves [11] and collision avoidance [12]. Calibrated car-following models have proven to be a valuable tool for assessing impacts of ICE-ACC vehicles via microscopic traffic simulations [4], [5], [7], [13]-[15]. Similar calibration approaches could be applied to the EV-ACC vehicles using experimental data. Although research has validated car-following models for ICE-ACC dynamics [15]–[17], it remains unclear whether these models can accurately represent real-world EV-ACC vehicles behavior. It is important to have car-following models that are customized to accurately reflect the car-following dynamics of EV-ACC vehicles. With this change in mind, the contributions of this study are three-fold:

- Proposing a new car-following model, namely EVM, demonstrating that it can capture the car-following behavior of EV-ACC vehicles better than commonly used ACC car-following models designed for ICE vehicles.
- Calibration of the EVM model parameter values that may contribute to the transportation community for future use in simulation-based studies.
- Examination and comparison of the performance of car-following models in traffic wave amplification in a string of EV-ACC vehicle simulation.

A. Zare, M. Shang, and R. Stern are with the Department of Civil, Environmental, and Geo-Engineering at the University of Minnesota, MN 55455, USA (email: {zare0032, shang140, rstern}@umn.edu).

X. D. Kan is with the Department of Civil, Environmental, and Geomatics Engineering at Florida Atlantic University, FL 33431, USA (email: kanx@fau.edu).

The remainder of this article is outlined as follows. First, we review the background on car-following models. Next, we propose a novel car-following model for EV-ACC vehicles that can capture the unique behavior of EVs in car-following. To obtain the parameter values, we introduce the experimental data used for this study. Then, the simulation process and the calibration approach are presented, and the calibration results for different car-following models are compared. Moreover, we show that the EVM model shows a more string-stable velocity than the commonly used car-following models. In the end, we conclude that the EVM model can simulate the behavior of EV-ACC vehicles better than commonly used car-following models, and future study opportunities are presented.

### II. CAR-FOLLOWING DYNAMICS

In this section, we review the general function that is utilized to simulate the car-following behavior of the EV ACC. We will then review two commonly used car-following models in the transportation community, which are used as a reference for model comparison.

## A. General function

Concepts of general microscopic car-following models were introduced in the 1950s [18] to understand the driving dynamics of individual vehicles. While numerous forms of car-following models have been developed, the underlying idea of car-following models remains that the acceleration or speed of a vehicle is a function of the following vehicle and its surroundings.

The general car-following model is given by Equation (1), which is an ordinary differential equation that describes the acceleration a(t) of a following vehicle is modeled with the inter-vehicle spacing s(t), the speed of the following vehicle v(t), and the relative speed between the vehicles  $\Delta v(t)$  at time t. Specifically, s(t) is the distance between the front bumper of the following vehicle and the rear bumper of the lead vehicle. The relative speed,  $\Delta v(t) = v_{\ell}(t) - v(t)$ , measures the difference in speed between the lead vehicle and the following vehicle. For brevity, we refer to the variables without explicit time index in the following sections.

$$a(t) = f(s(t), v(t), \Delta v(t)). \tag{1}$$

# B. Intelligent driver model (IDM)

The intelligent driver model [12] is designed to describe human-driven behavior, which can fully capture both the acceleration process and deceleration process. While the IDM has been extensively utilized in previous studies such as [19], [20] to model human-driven dynamics, it is also capable of accurately capturing the vehicle dynamics of the ICE-ACC vehicles [5], [7], [15], [21]. The IDM is mathematically represented as follows:

$$a = \alpha \left( 1 - \left( \frac{v}{v_0} \right)^{\delta} - \left( \frac{\hat{s}(v, \Delta v)}{s} \right)^2 \right) \tag{2}$$

$$\hat{s}(v, \Delta v) = s_0 + \tau v - \frac{v\Delta v}{2\sqrt{\alpha\beta}} \tag{3}$$

This model contains diverse parameter values  $\theta_{\rm IDM} = [v_0, \tau, \delta, s_0, \alpha, \beta]^{\top}$  to represent different car-following behavior. Each model parameter in  $\theta_{\rm IDM}$  holds a distinct physical interpretation:  $v_0$  is the desired speed;  $\tau$  represents time headway;  $\delta$  is an acceleration exponent;  $s_0$  denotes the stopping distance indicating the minimum spacing to the lead vehicle when stopping;  $\alpha$  and  $\beta$  are upper limits for vehicle acceleration and deceleration for a comfortable deceleration rate, respectively. The IDM can accurately simulate vehicle driving behavior by identifying model parameter values.

#### C. Optimal velocity, relative velocity (OVRV)

The optimal velocity, relative velocity car-following model has been widely used for modeling the dynamics of ICE-ACC vehicles [22], [23], displaying precision in characterizing their car-following behaviors [14], [24], [25]. The OVRV model is given by:

$$a = k_1 (s - \eta - \tau v) + k_2 (v_l - v), \tag{4}$$

The model parameters are  $\boldsymbol{\theta}_{\text{OVRV}} = [k_1, k_2, \eta, \tau]^{\top}$ . Of note,  $k_1$  represents the velocity gain, and  $k_2$  represents the velocity difference gain. Parameters  $\tau$  and  $\eta$  represent the time headway and stopping distance, respectively. The OVRV model can accurately reproduce ICE-ACC vehicle driving behavior by identifying  $k_1$ ,  $k_2$ ,  $\eta$ , and  $\tau$ .

#### III. ELECTRIC VEHICLE MODEL (EVM)

In this section, we initially introduce the experimental data used in this study. Then, we explain the difference between EV-ACC and ICE-ACC vehicles in car-following behavior by showing the spacing and speed trajectories of these vehicles in car-following. Then, the procedure for developing the new car-following model (EVM) and its formulation is presented.

#### A. Data

The EV-ACC vehicle trajectory data are adopted from [26] that Dr. X. D. Kan and his team collected from a series of carfollowing field experiments with a commercially available EV-ACC vehicle. More details about data collection can be found in [26].

The EV-ACC car following datasets consist of vehicle trajectories at different time gap settings, namely short, medium, long, and ex-long settings. The short setting means the EV-ACC vehicle follows the lead vehicle at the closest following gap, while the ex-long (i.e., extra-long) setting keeps the furthest following gap from the preceding vehicle. The medium setting and long setting represent the following gap of an EV-ACC vehicle that is operated between the shortest setting and the ex-long setting.

#### B. Exploration of EV-ACC car-following behavior

The sample speed trajectory data of an EV following a lead car is presented in Figure 1a. In the example shown, the EV accelerates to a slightly higher speed than the lead vehicle. The EV maintains this speed for an extended period, slowly catching up to the lead vehicle and resulting in a decrease in the gap between them ( $\Delta v < 0$ ) (between seconds 35 to 60). The main reason for this distinct behavior is that EVs

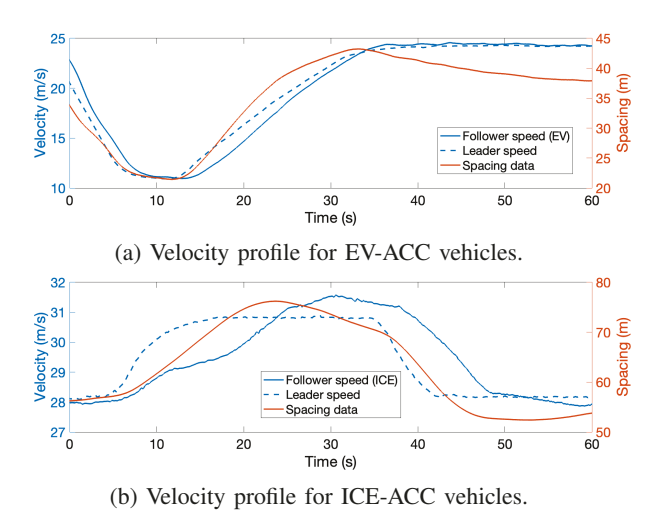


Fig. 1: Sample velocity trajectory profiles for EV-ACC vehicles and ICE-ACC vehicles. A unique driving behavior is observed that the EV-ACC vehicles accelerate or decelerate more rapidly than the ICE-ACC vehicles, resulting in different spacing gaps between vehicles.

accelerate more rapidly at the beginning due to their instant torque, and the spacing between the leader and follower is not as large as ICE vehicles (i.e., EVs catch up with the lead vehicle much faster). As seen in Figure 1b, the initial acceleration is more gradual for ICE vehicles than EVs, leading to a much larger spacing gap. As a result, ICE vehicles attempt to increase speed to catch up with the lead vehicle. This unique behavior in EVs motivates the development of a new car-following model that can specifically describe the unique car-following behavior of EVs.

## C. Formulation of EVM

Mechanically, accelerating and braking involve distinct processes for a car. To enhance the accuracy of the carfollowing model, we can consider separate phases based on the relative speed, and specify distinct following dynamics within each phase. In contrast to earlier symmetric models discussed in section II that rely on a single function, asymmetric car-following models [27]–[29] differentiate between acceleration and deceleration phases and specify distinct car-following dynamics for each. Accounting for the asymmetry between accelerating and braking allows a more realistic characterization of vehicle dynamics.

Specifically, inspired by the asymmetric OVRV (AOVRV) model [17], we split the acceleration into three phases in order to build an accurate model for the EVs. The EV model is given by:

$$a = \begin{cases} a_D = k_1(s - \eta - \tau v) + k_{2D}\Delta v, & \Delta v q. \end{cases}$$
 (5)

In the EVM, parameters  $\tau$  and  $\eta$  are as defined in Equation (4). Parameters  $k_{2A}$  and  $k_{2D}$  denote relative velocity gain for EV acceleration and deceleration, respectively. It

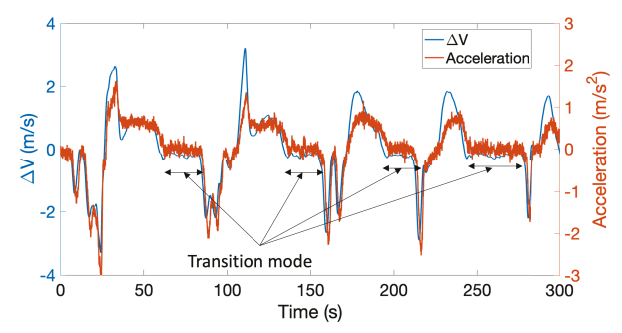


Fig. 2: Acceleration of the following vehicle versus the relative speed of the vehicles. During the transition mode, when the acceleration oscillates around zero, the relative speed of the vehicles also oscillates within a range of -0.2 to 0.1.

should be noted that the parameter  $k_1$  signifies optimal velocity gain for both acceleration and deceleration driving modes. We assume a single parameter for the optimal velocity gain for both acceleration and deceleration to minimize the disturbance in the acceleration value when it is moving between the criteria around zero, which is based on the assumption that the acceleration  $(a_A)$  and deceleration  $(a_D)$  terms are equal when  $\Delta v \approx 0$  (m/s).

As shown in Figure 2 when the relative speed  $\Delta v < -0.2$  (m/s) and  $\Delta v > 0.1$  (m/s), the EV is operated with a deceleration mode and acceleration mode, which are denoted with  $a_D$  and  $a_A$ , respectively. When  $-0.2 \leq \Delta v \leq 0.1$  (m/s), the acceleration of the following vehicle is oscillating around zero. We define a transition mode  $a_T$  with a constant acceleration d to capture this unique feature of EV behavior. The introduction of  $a_T$  is motivated by the observation of EV trajectories that have roughly constant velocity (i.e., very small constant acceleration close to zero) during the car following process as discussed in Section III-B.

The criteria for the transition mode (p and q values) in Equation (5) is obtained by evaluating the spacing root mean square error (RMSE) with different p, q values between -0.2 m/s and 0.1 m/s. We determine the criteria with the lowest spacing RMSE when p = -0.1 m/s and q = -0.05 m/s.

## IV. MODEL CALIBRATION

In this section, we initially present the simulation procedure. Then, the calibration approach used to acquire vehicle dynamics is discussed, and the calibrated parameter values for the EVM model are presented.

#### A. Model simulation

The vehicle dynamics are simulated using a forward Euler's method in this paper. This process involves breaking down the continuous time model into discrete time steps  $\Delta t$ :

$$\begin{bmatrix} s \\ v \end{bmatrix}_{t+\Delta t} = \begin{bmatrix} s \\ v \end{bmatrix}_t + \begin{bmatrix} \Delta v \\ a \end{bmatrix}_t \Delta t, \tag{6}$$

where s, v, a, and  $\Delta v$  are defined above.

## B. Calibration approach

Various techniques for determining the best-fit parameter values are discussed in [30]. However, the transportation community typically prefers batch optimization as their preferred approach [15], [17], [21]. To obtain the optimal parameters  $\theta$ , we use a calibration method that involves minimizing the RMSE between simulated trajectories and experimental data.

Parameter values are initially guessed in the batch calibration process. Next, we generate simulated trajectories using the current candidate parameter values. Then, we compare these simulated trajectories to the experimental data and calculate the spacing RMSE. Finally, we use the gradient descent optimization approach to update the parameter values until the simulated trajectories are comparable to the observed experimental trajectory data, resulting in the best-fit model parameter values.

To find the best-fit model parameter values for EV-ACC vehicles, we slice the dataset into three subsets that are 100 s long and use these sliced datasets for training purposes. Then, we test the model performance on the entire dataset. This is done to avoid data over-fitting.

#### C. Calibration results

We present The EVM model's parameter values in Table I. The presented model parameters in Table I are the best-fit models with the lowest RMSE under different gap settings. The RMSE value of these models are presented in the next section in Table II along with the RMSE value for the IDM and OVRV models fitted on the EV-ACC data.

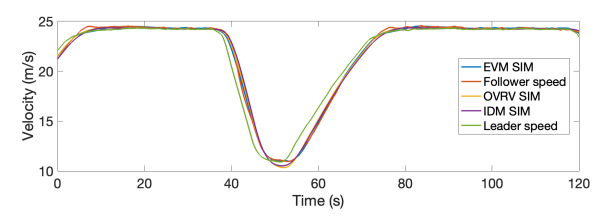
Gap setting	$k_1 \ (s^{-2})$	$\begin{array}{c} k_{2D} \\ (s^{-1}) \end{array}$	$\begin{array}{c} k_{2A} \\ (s^{-1}) \end{array}$	$d (m/s^2)$	$\tau$ $(s)$	$\eta$ $(m)$
Short	0.244	0.339	0.286	0.319	1.000	10.287
Medium	0.092	0.662	0.283	0.074	1.118	12.177
Long	0.124	0.457	0.272	0.116	1.501	11.012
Ex-long	0.175	0.279	0.150	0.269	2.093	8.399

TABLE I: Parameter values for different gap settings in the EVM.

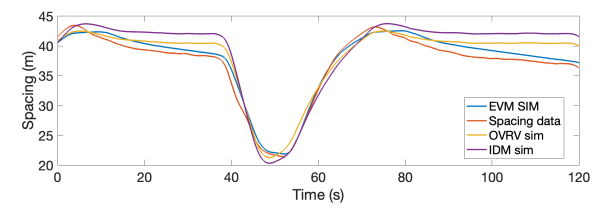
## V. MODEL COMPARISON RESULTS

To showcase the performance of the EVM model, we reproduce the speed and spacing of the following vehicle using the parameter values of the best-fit model for the EVM, IDM, and OVRV. Figures 3 and 4 represent the simulated trajectories alongside the speed and spacing trajectories in the experimental data for the medium and long gap settings.

Figures 3a and 4a display the simulated speed trajectories. A closer inspection reveals minor inconsistencies in OVRV and IDM when the deceleration is finished and the lead vehicle starts to accelerate. However, all models are able to accurately capture the EV-ACC following speed. It should be noted that EVM reproduces the EV-ACC inter-vehicle spacing more accurately than IDM and OVRV as it is shown in Figures 3b and 4b. In particular, in transition mode, the EVM reproduces spacing more accurately when following and leading vehicles travel at a steady speed, as a result of the linear phase in the EVM acceleration ( $a_T$  in Equation 5).

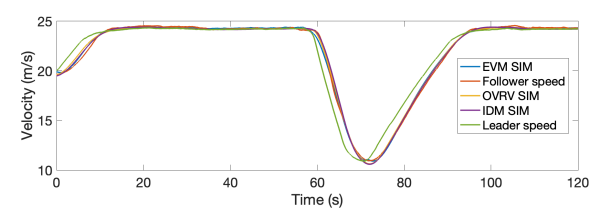


(a) The IDM, OVRV, and EVM simulation on the speed of the following vehicle for medium gap setting.

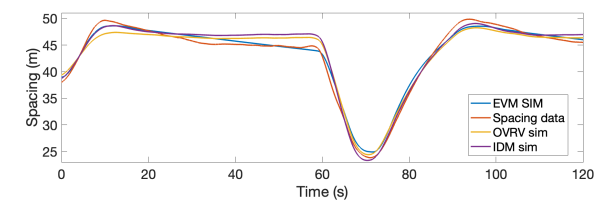


(b) The IDM, OVRV, and EVM simulation on the spacing of the following vehicle for medium gap setting.

Fig. 3: Performance comparison of IDM, OVRV, and EVM on the data of the medium gap setting.



(a) The IDM, OVRV, and EVM simulation on the speed of the following vehicle for long gap setting.



(b) The IDM, OVRV, and EVM simulation on the spacing of the following vehicle for long gap setting.

Fig. 4: Performance comparison of IDM, OVRV, and EVM on the data of the long gap setting.

This occurs when the relative speed of vehicles  $(\Delta v)$  is close to zero. The acceleration value in the transition mode (d) in Table I represents the calibrated value for the linear acceleration part. A small positive value for d indicates that the following vehicle is smoothly approaching the lead vehicle.

To numerically compare the performance of the EVM model with IDM and OVRV, we calculate the spacing RMSE using the experimental data and the simulated spacing trajectories. Table II presents the RMSE values for the best-fit models under different gap settings. It is clear from the numerical comparison of RMSE that the EVM outperforms both the IDM and OVRV models in all gap settings.

Comparing the RMSE value obtained from simulating the medium gap setting's spacing trajectory, we can observe that the EVM model outperforms the IDM and the OVRV model

Gap setting	Spacing RMSE (m)			EVM RMSE change (%)		
	EVM	IDM	OVRV	IDM	OVRV	
Short	1.771	2.758	2.211	-56%	-24%	
Medium	1.265	1.897	1.756	-50%	-39%	
Long	1.190	1.316	1.319	-11%	-11%	
Ex-long	1.354	1.423	1.575	-5%	-16%	

TABLE II: RMSE values for different gap settings in EVM, IDM, and OVRV.

by reducing spacing RMSE by 50% and 39%, respectively. The benefits of the EVM can be observed in Figure 3b, where the EVM simulated spacing more closely follows the spacing data than the OVRV model and IDM between 10-40 seconds and 80-120 seconds, when the following vehicle is smoothly approaching the lead vehicle. Similarly, based on the comparison of RMSE values of different models for the long gap setting, the EVM outperforms IDM and OVRV by 11%. The slightly better performance of the EVM can be observed in Figure 4b between 10-60 seconds. We find that that the EVM outperforms commonly used carfollowing models in describing the linear acceleration of EV-ACC vehicles. As mentioned earlier, this particular behavior is uniquely observed in EV-ACC vehicles.

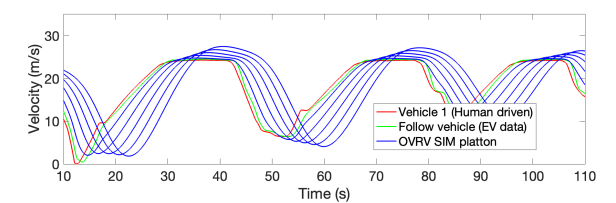
#### VI. SIMULATION OF A PLATOON OF EV-ACC VEHICLES

String stability refers to whether a disturbance from an equilibrium state will amplify or attenuate along a string of vehicles. Small fluctuations in velocity can propagate upstream through vehicle interactions [31]. Specifically, string instability occurs if disturbances grow along the string. Conversely, if all disturbances decrease along the string, the system is considered to be string stable. There are several methods to analyze the string stability of a flow numerically [32]–[34]. However, analyzing the string stability of the EVM model is a complex mathematical problem, and we leave it for future work. Instead, we simulate a string of 5 vehicles following their front vehicle as shown in Figure 5 based on the parameter value of the best-fit model of EVM, IDM, and OVRV model. The lead vehicle and the first following vehicle's driving behavior are taken from experimental data, while the other five EVs' car-following behavior is simulated using calibrated parameter values in the models. This platoon simulation is based on the assumption that all the EVs have similar braking and acceleration limits. Through this simulation, we gain a better understanding of how traffic flow may be affected by EV-ACC vehicles behaving based on the EVM model in comparison to IDM and OVRV.

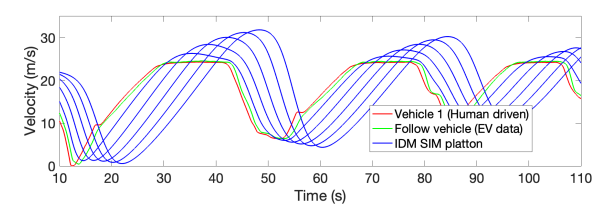
Figure 6 shows the string of EV-ACC vehicles behaving based on the parameter values of the OVRV, IDM and EVM model, respectively. Notably, when comparing Figure 6b to Figure 6c, we find the amplification of the speed disturbances with the IDM model is much more significant than the EVM in acceleration. While Figures 6a and 6c show the amplification is slightly less for the EVM model, both models show a string stability in acceleration.



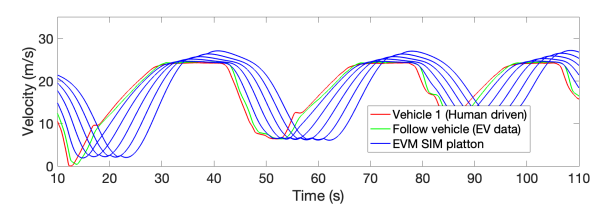
Fig. 5: Platoon of vehicles in string stability simulation showing a human-driven vehicle being followed by an EV (data) and a simulated platoon of 5 EVs with similar braking and acceleration limits.



(a) Simulation of a string of EV-ACC vehicles using the OVRV model.



(b) Simulation of a string of EV-ACC vehicles using the IDM model.



(c) Simulation of a string of EV-ACC vehicles using the EVM model.

Fig. 6: Simulation of a string of vehicles with the calibrated parameter values in Table I for EV-ACC vehicles. (a), (b), and (c) are simulations with the OVRV, IDM, and EVM models, respectively.

Comparing Figures 6a, 6b, and 6c highlights that the OVRV and EVM models exhibit a more stable string behavior. However, the EVM model shows less amplification than the OVRV model, particularly during seconds 50-60. To this end, the EVM model shows a more realistic amplification in simulating a string of EV-ACC vehicles compared to the OVRV model and the IDM.

## VII. CONCLUSION AND FUTURE WORK

This study introduces the Electric Vehicle Model (EVM), a novel microscopic car-following model to explain the dynamics of EV-ACC car-following behavior. During the EV-ACC car-following, the EV accelerates to a slightly higher speed than the lead vehicle once the acceleration is complete. It then maintains this speed for an extended period, slowly closing the gap between the vehicles in a linear manner. This phenomenon is not observed in ICE vehicles under

the same circumstances. Compared to commonly used carfollowing models, IDM and OVRV, EVM performs better in simulating the linear drop in spacing when the lead vehicle maintains a constant speed. The parameters of the model are calibrated using data of an experiment carried out on commercially available EV-ACC vehicles. In addition, the simulated spacing and speed in the EVM are compared to IDM and OVRV. The results show that the EVM outperforms IDM and OVRV in all of the gap settings, specifically in tracking the spacing linear drop when the relative speed  $(\Delta v)$  of vehicles is almost zero.

Moreover, results of simulating a platoon of EV-ACC vehicles show that EV-ACC vehicles behaving based on parameter values of the EVM model have the potential to minimize the amplification of traffic waves in comparison to the IDM and OVRV models. For future works, the impacts of EV-ACC vehicles using the EVM model on traffic flow and fundamental diagram can be explored. Moreover, it would be interesting to investigate the potential impact of a mixed powertrain environment where ICE vehicles and EVs coexist.

#### REFERENCES

- A. Talebpour and H. S. Mahmassani, "Influence of autonomous and connected vehicles on stability of traffic flow," in *Transportation Research Board 94th Annual Meeting*, no. 15-5971, 2015.
- [2] R. E. Stern, S. Cui, M. L. Delle Monache, R. Bhadani, M. Bunting, M. Churchill, N. Hamilton, H. Pohlmann, F. Wu, B. Piccoli et al., "Dissipation of stop-and-go waves via control of autonomous vehicles: Field experiments," *Transportation Research Part C: Emerging Technologies*, vol. 89, pp. 205–221, 2018.
- [3] SAE, "Society of Automotive Engineers J3016: Taxonomy and Definitions for Terms Related to Driving Automation Systems for On-Road Motor Vehicles," Standard, June 2018.
- [4] L. C. Davis, "Effect of adaptive cruise control systems on traffic flow," Physical Review E, vol. 69, no. 6, p. 066110, 2004.
- [5] A. Talebpour and H. S. Mahmassani, "Influence of connected and autonomous vehicles on traffic flow stability and throughput," *Trans*portation Research Part C: Emerging Technologies, vol. 71, pp. 143– 163, 2016.
- [6] Y. Qin, H. Wang, and B. Ran, "Stability analysis of connected and automated vehicles to reduce fuel consumption and emissions," *Journal of Transportation Engineering, Part A: Systems*, vol. 144, no. 11, p. 04018068, 2018.
- [7] M. Shang and R. Stern, "Impacts of commercially available adaptive cruise control vehicles on highway stability and throughput," Transportation Research Part C: Emerging Technologies, vol. 122, p. 102897, 2021.
- [8] J. Vander Werf, S. E. Shladover, M. A. Miller, and N. Kourjanskaia, "Effects of adaptive cruise control systems on highway traffic flow capacity," *Transportation Research Record*, vol. 1800, no. 1, pp. 78– 84, 2002.
- [9] D. C. Gazis, R. Herman, and R. B. Potts, "Car-following theory of steady-state traffic flow," *Operations Research*, vol. 7, no. 4, pp. 499– 505, 1959.
- [10] M. Aycin and R. Benekohal, "Comparison of car-following models for simulation," *Transportation research record*, vol. 1678, no. 1, pp. 116–127, 1999.
- [11] M. Bando, H. K., A. Nakayama, A. Shibata, and Y. Sugiyama, "Dynamical model of traffic congestion and numerical simulation," *Physical Review E*, vol. 51, no. 2, pp. 1035–1042, 1995.
- [12] M. Treiber, A. Hennecke, and D. Helbing, "Congested traffic states in empirical observations and microscopic simulations," *Physical Review E*, vol. 62, no. 2, p. 1805, 2000.
- [13] L. C. Davis, "The effects of mechanical response on the dynamics and string stability of a platoon of adaptive cruise control vehicles," *Physica A: Statistical Mechanics and its Applications*, vol. 392, no. 17, pp. 3798–3805, 2013.

- [14] G. Gunter, D. Gloudemans, R. Stern et al., "Are commercially implemented adaptive cruise control systems string stable?" *IEEE Transactions on Intelligent Transportation Systems*, vol. 22, no. 11, pp. 6992–7003, 2020.
- [15] G. Gunter, R. Stern, and D. Work, "Modeling adaptive cruise control vehicles from experimental data: model comparison," in 2019 IEEE Intelligent Transportation Systems Conference (ITSC). IEEE, 2019, pp. 3049–3054.
- [16] V. Milanés, S. E. Shladover, J. Spring et al., "Cooperative adaptive cruise control in real traffic situations," *IEEE Transactions on Intelli*gent Transportation Systems, vol. 15, no. 1, pp. 296–305, 2014.
- [17] M. Shang, B. Rosenblad, and R. Stern, "A novel asymmetric car following model for driver-assist enabled vehicle dynamics," *IEEE Transactions on Intelligent Transportation Systems*, 2022.
- [18] L. A. Pipes, "An operational analysis of traffic dynamics," *Journal of applied physics*, vol. 24, no. 3, pp. 274–281, 1953.
- [19] A. Kesting, M. Treiber, M.and Schönhof, and D. Helbing, "Adaptive cruise control design for active congestion avoidance," *Transportation Research Part C: Emerging Technologies*, vol. 16, no. 6, pp. 668–683, 2008
- [20] M. Shang and R. Stern, "Calibrating heterogeneous car-following models for human drivers in oscillatory traffic conditions," in 2020 Forum on Integrated and Sustainable Transportation Systems (FISTS). IEEE, 2020, pp. 101–106.
- [21] F. De Souza and R. E. Stern, "Calibrating microscopic model for commercially available autonomous driving systems: a multi-objective approach," in *Transportation Research Board Annual Meeting*, 2019.
- [22] R. Rajamani, Vehicle dynamics and control. Springer Science & Business Media, 2011.
- [23] P. Ioannou and C. Chien, "Autonomous intelligent cruise control," IEEE Transactions on Vehicular Technology, vol. 42, no. 4, pp. 657–672, 1993.
- [24] V. Milanés and S. E. Shladover, "Modeling cooperative and autonomous adaptive cruise control dynamic responses using experimental data," *Transportation Research Part C: Emerging Technologies*, vol. 48, pp. 285–300, 2014.
- [25] G. Gunter, C. Janssen, W. Barbour, R. Stern, and D. Work, "Model based string stability of adaptive cruise control systems using field data," *IEEE Transactions on Intelligent Vehicles*, vol. 5, no. 1, pp. 90–99, 2019.
- [26] S. Lapardhaja, K. U. Yagantekin, M. Yang, T. A. Majumder, X. Kan, and M. Badhrudeen, "Unlocking potential capacity benefits of electric vehicles (evs) with adaptive cruise control (acc)," *Transportmetrica B: Transport Dynamics*, vol. 11, no. 1, pp. 1894–1911, 2023.
- [27] H. Gong, H. Liu, and B. Wang, "An asymmetric full velocity difference car-following model," *Physica A: Statistical Mechanics and its Applications*, vol. 387, no. 11, pp. 2595–2602, 2008.
- [28] X. Xu, J. Pang, and C. Monterola, "Asymmetric optimal-velocity carfollowing model," *Physica A: Statistical Mechanics and its Applica*tions, vol. 436, pp. 565–571, 2015.
- [29] A. Jafaripournimchahi, W. Hu, and L. Sun, "An asymmetricanticipation car-following model in the era of autonomous-connected and human-driving vehicles," *Journal of Advanced Transportation*, vol. 2020, 2020.
- [30] Y. Wang, G. Gunter, M. Nice, M. Delle Monache, and D. Work, "Online parameter estimation methods for adaptive cruise control systems," *IEEE Transactions on Intelligent Vehicles*, vol. 6, no. 2, pp. 288–298, 2020.
- [31] Y. Sugiyama, M. Fukui, M. Kikuchi, K. Hasebe, A. Nakayama, K. Nishinari, S.-i. Tadaki, and S. Yukawa, "Traffic jams without bottlenecks—experimental evidence for the physical mechanism of the formation of a jam," *New journal of physics*, vol. 10, no. 3, p. 033001, 2008.
- [32] M. Bando, K. Hasebe, A. Nakayama, A. Shibata, and Y. Sugiyama, "Dynamical model of traffic congestion and numerical simulation," *Physical review E*, vol. 51, no. 2, p. 1035, 1995.
- [33] T.-S. Chow, "Operational analysis of a traffic-dynamics problem," Operations Research, vol. 6, no. 6, pp. 827–834, 1958.
- [34] R. Liu and X. Li, "Stability analysis of a multi-phase car-following model," *Physica A: Statistical Mechanics and its Applications*, vol. 392, no. 11, pp. 2660–2671, 2013.